PROCEEDINGS OF SCIENCE

Microphysics of electron acceleration and heating at nonrelativistic perpendicular shocks of young supernova remnants

Artem Bohdan*
DESY, Platanenallee 6, 15738 Zeuthen, Germany
E-mail: artem.bohdan@desy.de

Martin Pohl
Institute of Physics and Astronomy, University of Potsdam, Karl-Liebknecht-Strasse 24/25, 14476 Potsdam, Germany
DESY, Platanenallee 6, 15738 Zeuthen, Germany

Jacek Niemiec
Institute of Nuclear Physics Polish Academy of Sciences, PL-31342 Krakow, Poland

Takanobu Amano, Masahiro Hoshino
Department of Earth and Planetary Science, University of Tokyo, 7-3-1 Hongo, Tokyo 113-0033, Japan

Yosuke Matsumoto
Department of Physics, Chiba University, 1-33 Yayoi, Inage-ku, Chiba 263-8522, Japan

Particle injection is one of the most troublesome and still unresolved issues of the theory of diffusive shock acceleration (DSA) of galactic cosmic rays. Supernova remnants harbor non-relativistic collisionless shocks with high Alfven and sonic Mach numbers. To accelerate electrons up to the injection energy, a shock-internal acceleration mechanism is required. We present results of two-dimensional fully kinetic particle-in-cell simulations of perpendicular shocks with different values of Mach numbers and ion-to-electron mass ratios. Such systems are known as supercritical shocks, in which the shock potential is capable to reflect portion of upcoming ions upstream. In weakly magnetized plasmas that leads to the excitation of the electrostatic Buneman instability in the shock foot and to the formation of magnetic filaments in the shock ramp, resulting from the ion-beam-Weibel instability. These instabilities are responsible for electron acceleration via shock surfing acceleration and magnetic reconnection. The individual impact of these acceleration processes on the production of non-thermal electrons is discussed here. They strongly depend on the Mach number and ion-to-electron mass ratio, which is critical for predicting the electron injection efficiency at shocks with realistic physical parameters. The redistribution of ion bulk kinetic energy into ion thermal, electron thermal and magnetic field energies in the shock transition are also considered here.

36th International Cosmic Ray Conference -ICRC2019-
July 24th - August 1st, 2019
Madison, WI, U.S.A.

*Speaker.

PoS(ICRC2019)200

1. Nonrelativistic perpendicular shocks

Supernova remnant (SNR) shocks are known as a source of galactic cosmic rays which are accelerated via diffusive shock acceleration (DSA), also known as first order Fermi acceleration. However electron injection into DSA is still an issue. SNR shock are nonrelativistic and characterized by high Alfven and sonic Mach numbers. Theoretical studies of these shocks in perpendicular configuration demonstrate a great importance of the reflected ions in the structure of such shocks. Reflected ions interact with the incoming plasma and produce two instabilities in the shock transition: electrostatic Buneman instability at the leading edge of the shock foot (Fig. 1c) and Weibel-type filamentation instability in the foot-ramp region (Fig. 1b). The Buneman instability results from the interaction of the shock-reflected ions with the incoming electrons. Electrostatic waves can capture electrons which can be accelerated by convective electric field up to relativistic energy if the trapping condition is satisfied [1]. This acceleration mechanism is known as shock surfing acceleration (SSA) and its efficiency strongly depends of the setup and physical parameters [2, 3]. The Weibel-type instability is excited because of interaction of shock reflected and incoming ions. The incoming magnetic field lines are strongly deformed through the Weibel instability forming appropriate conditions for magnetic reconnection [4]. Magnetic reconnection refers to the change of magnetic field topology and converts the magnetic energy to the kinetic energy of particles through number of processes [5].

2. Simulation setup

The simulation is performed by usage of the flow-flow method. It considers an interaction of two counterstreaming electron-ion plasma flows. As a result of the two plasma slabs collision

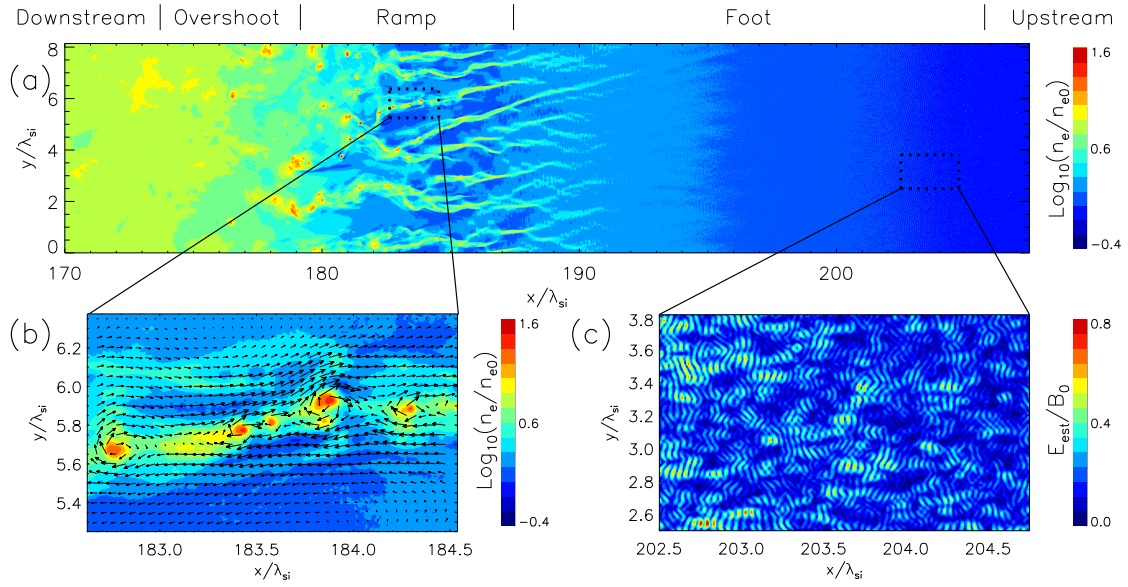

Figure 1: The structure of high Mach number perpendicular shock: (a) - electron density in the shock region; (b) - electron density with overlapped in-plane component of magnetic field in magnetic reconnection region; (c) - electrostatic field strength in the Buneman instability region. λ_{si} is the ion skin length.

two shocks are formed propagating in opposite directions. The homogeneous magnetic field, $\mathbf{B}_0$, is perpendicular to the shock normal and parallel to the y-axis, so-called in-plane configuration. The particle-in-cell (PIC) code we use is a 2D3V-modified and MPI-parallelized version of the relativistic electromagnetic PIC code TRISTAN [6, 7].

The resulting shock velocity in all simulations is $v_{sh} \approx 0.26c$, where c is the speed of light. Parameters of simulations cover wide range of the ion-to-electron mass ratios ($m_i/me = 50-400$) and Alfvénic Mach number values, $M_A = 23-69$, which allows us to estimate scaling of different injection mechanisms up to the realistic parameters. Here we discuss only results for one of the shocks from each run, namely, shocks propagating in plasma with the plasma beta (the ratio of the plasma pressure to the magnetic pressure) $\beta = 0.5$. The simulation parameters a listed in Table 1.

3. Formation of a high energy tail

Our previous study [3] suggests that the downstream nonthermal population of electrons strongly correlates with an efficiency of the pre-aceleration via SSA in the Buneman zone. However further interaction of electrons with turbulent Weibel region and magnetic reconnection sites may change that picture. Figure 2 illustrates the temporal evolution of the average energy for a selected electron population that traverses the shock structure. This analysis is based on tracing data of about $5 \cdot 10^5$ individual particles for the simulation with $m_i/m_e = 200$ and $M_A = 45$ (run E). The traced particles are in upstream region at $t1$, at time $t2$ they just crossed the Buneman wave region, thus the electron energy distribution consists of thermal bulk and nonthermal population. At time $t3$ the electrons reach the turbulent Weibel region and finely they are in the downstream at time $t4$. Two subsets of electrons are chosen for the analysis:

- The first subset is defined at time t_2 and consists of electrons that have been pre-accelerated in the Buneman instability region and populate the nonthermal tail in the spectrum. For this

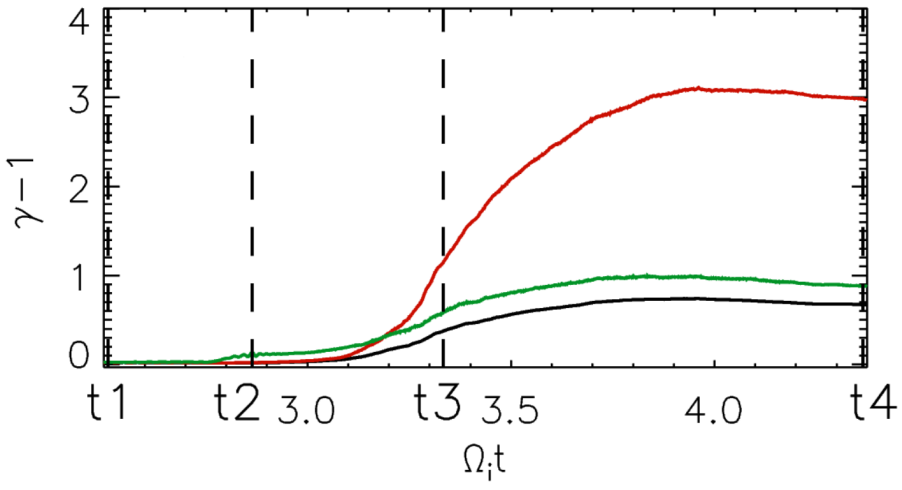

Figure 2: Evolution of the average energy of traced electrons. Black line refers to all traced electrons, green lines correspond to electrons energized in the Buneman zone, and red lines are for high-energy electrons downstream of the shock. The dashed lines are time markers for t1-t4.

subset we chose particles with kinetic energies higher than $(\gamma-1) > 0.1$. Their energy is shown with green solid line.

- The second subset form electrons that at time t_4 have energies $(\gamma-1) > 5k_BT/(m_ec^2)$, where T is the downstream temperature derived for the distribution of traced electrons. This subset represents nonthermal electrons in the downstream region. Their energy is marked with red solid line.

The green population in energized in the Buneman zone via SSA ($t2$) and further energization is commensurate with the average heating rate (black line). The red subset is strongly accelerated in the Weibel instability region and where magnetic reconnection occurs, which suggest strong influence of magnetic reconnection and chaotic Fermi-like acceleration processes. The intersection of the green and red electron subsets explicitly defines the influence of the Buneman instability on the formation of the nonthermal tails. In the current particle sample, only 5% of BI electrons can be found in the HE electron subset. Analysis of all simulation shows that the nonthermal electron fraction produced via SSA (NTEF_{SSA}) is smaller for higher ion-to-electron mass ratios because of stronger heating in the shock foot-ramp while SSA efficiency remains approximately constant for the range of parameters considered here.

Magnetic reconnection produces substantial part of nonthermal electrons for large mass ratio and becomes a dominant acceleration process (see NTEF_{MR} in Table 1). In this case Weibel instability develops faster and almost all the Weibel filaments undergo magnetic reconnection. Therefore almost all particles are involved in magnetic reconnection in runs with high Alfven Mach numbers and ion-to-electron mass ratios. Remaining nonthermal electron fraction which is not covered by SSA or magnetic reconnection is treated as electrons associated with chaotic second-order Fermi-like acceleration process only.

4. Energy redistribution

Far upstream ions carry most of the total plasma energy in weakly magnetized plasmas. In the shock transition ion kinetic energy is strongly redistributed. In the downstream region, where bulk ion and electron energies are negligible, the energy is distributed among thermal ions, thermal electrons and the magnetic field. The energy of the electric field is negligible. Thermal electrons keep about $(5-9)\%$ of the upstream ion kinetic energy and this fraction is independent of the mass ratio and Mach number. About $(2-5)\%$ of energy goes to the downstream magnetic field and the fraction is smaller for larger mass ratios. The normalized downstream magnetic field energy is larger for shocks with higher Alfven Mach numbers, namely $B^2_{down}/B_0 \approx 80$ for run A and $B^2_{down}/B_0 \approx 300$ for run F, thus substantial turbulence is generated in the shock transition.

5. Summary

Here we present results 2D3V PIC simulations of SNR shocks which cover wide range of physical and numerical parameters. This allows us to make reasonable predictions for the behaviour of these systems for the realistic parameters observed in SNRs. Our results can be summarized as follows:

Run	m_i/m_e	M_A	k_BT/m_ec^2	NTEF (%)	NTEF_{SSA} (%)	NTEF_{MR} (%)	f_{MR} (%)
A	50	23	0.09	0.28	0.15	0.1	10
B	100	32	0.18	0.55	0.05	0.4	26
C	100	46	0.22	0.36	0.05	0.13	38
D	200	32	0.3	0.7	0.025	0.55	38
E	200	45	0.37	0.56	0.025	0.5	43
F	400	69	0.73	0.57	0.0015	0.4	79

Table 1: m_i/m_e is the ion-to-electron mass ratio. M_A is the Alfvénic Mach number. k_BT/m_ec^2 is the temperature of the downstream electrons. NTEF is the nonthermal electron fraction in the shock downstream, which is defined as excess of electrons above Maxwellian fit. NTEF_{SSA} is the nonthermal electron fraction produced via SSA. NTEF_{MR} is the nonthermal electron fraction produced through magnetic reconnection. f_{MR} is the fraction of electrons involved in magnetic reconnection.

- Nonthermal electrons are mainly produced in ramp-overshoot region.
- Three acceleration mechanisms operate in the shock transition: SSA at the leading edge of the shock foot (Buneman instability region), acceleration via magnetic reconnection in the shock ramp (Weibel instability region), chaotic second-order Fermi-like acceleration in the shock foot and ramp (Weibel instability region).
- Growth rate and capability to accelerate electros via SSA and magnetic reconnection strongly depends on Mach number and mass ratio. In case of high M_A and m_i/m_e SSA become less important while magnetic reconnection dominates in production of nonthermal electrons.
- Almost all particles are involved in magnetic reconnection caused by Weibel filaments decay in case of large mass ratio.
- The same fraction ($\sim 7\%$) of the upstream ion kinetic energy goes to the thermal electrons. The normalized downstream magnetic field energy increases with Alfven Mach number of the shock.

Acknowledgments

The work of J.N. has been supported supported by Narodowe Centrum Nauki through research project DEC-2013/10/E/ST9/00662. This work was also supported by JSPS-PAN Bilateral Joint Research Project Grant Number 180500000671. Numerical simulations have been performed on the Prometheus system at ACC Cyfronet AGH. Part of the numerical work was also conducted on resources provided by The North-German Supercomputing Alliance (HLRN) under projects bbp00003 and bbp00014.

References

[1] Matsumoto, Y., Amano, T., & Hoshino, M. 2012, ApJ, 755, 109

[2] Bohdan, A., Niemiec, J., Pohl, M., et al. 2019, ApJ, 878, 5

[3] Bohdan, A., Niemiec, J., Kobzar, O., et al. 2017, ApJ, 847, 71

[4] Matsumoto, Y., Amano, T., Kato, T. N., & Hoshino, M. 2015, Science, 347, 974

[5] Bohdan, A., Niemiec, J., Kobzar, O., et al. 2017, International Cosmic Ray Conference, 301, 587

[6] Buneman, O. 1993, in *Computer Space Plasma Physics: Simulation Techniques and Software*, Eds.: Matsumoto & Omura, Tokyo: Terra, p.67

[7] Niemiec, J., Pohl, M., Stroman, T., & Nishikawa, K.-I. 2008, ApJ, 684, 1174-1189